

A Monolithic Ultra-compact InP O-CDMA Encoder with Planarization by HPVE Regrowth

J. Cao, R. G. Broeke, C. Ji, Y. Du, N. Chubun, P. Bjeletich, and S. J. B. Yoo
Department of Electrical and Computer Engineering, University of California, Davis, CA 95616, USA
Email: yoo@ece.ucdavis.edu

F. Olsson, S. Lourdudoss

Department of Microelectronics and Information Technology, Royal Institute of Technology, KTH-Electrum 229, S-16440 Kista, Sweden

P. L. Stephan

Lawrence Livermore National Laboratory, Livermore, CA 94550, USA

Abstract: We report a monolithic, ultra-compact optical-CDMA encoder/decoder photonic chip in InP with surface planarization by low-pressure Hydride-Vapor-Phase-Epitaxy regrowth. The chip consists of an AWG pair and eight electro-optic phase shifters and demonstrated excellent encoding operation.

©2005 Optical Society of America

OCIS codes: 060.4510 Optical communications, 230.3120 Integrated optics devices

1. Introduction

The Optical Code Division Multiple Access (O-CDMA) technology is potentially well suited for providing very flexible and high-capacity access to the vast networking capacity available in all-optical local area networks [1-2]. Configuration and reconfiguration of such access capacity are easily achieved based on code selection, instead of the wavelength or time-slotting based approach in WDM or TDM networks. In particular, local nodes in an all-optical network can independently select a desired code in the optical layer without involving central nodes, and thus simplifying the control and management of the local area networks. While the feasibility of O-CDMA has been demonstrated in free space optical systems [3], monolithic chip scale integration and miniaturization are essential for reliable operation and low-cost large scale adoption such systems. The key element in an O-CDMA system is the spectral phase encoder/decoder, for which AWGs are very attractive candidates due to their high spectral resolution. An AWG-based encoder using Si technology and a non-programmable external phase shifters has been previously reported [4]. This paper presents the first full monolithic AWG-based encoder in InP/InGaAsP. It incorporates a high-speed electro-optic phase shifter array for rapid code reconfigurations with negligible power consumption. Our approach is suitable for future higher level on-chip integration of even more functionalities in O-CDMA transmitters and receivers.

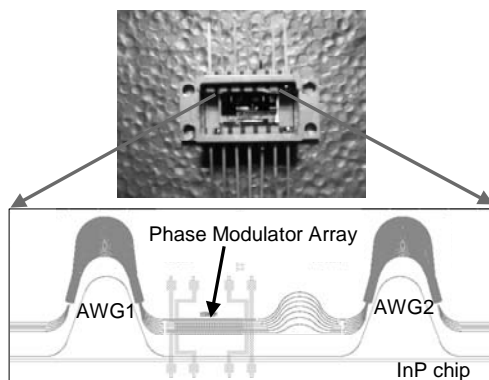


Fig. 1. A packaged O-CDMA encoder chip.

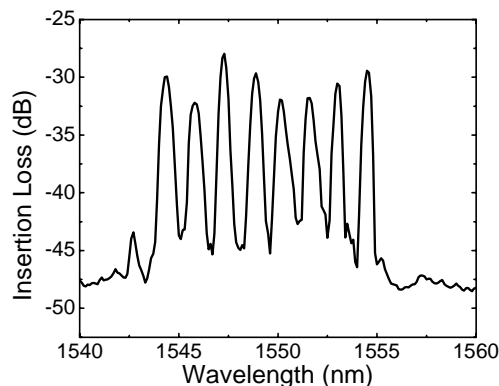


Fig. 2. Transmission spectrum of the encoder chip.

2. Operation Principle and Fabrication

A Spectral Phase Encoded Time Spreading (SPECTS)-OCDMA system uses spectrally encoded ultra-short pulses for data transmission [5]. Only the correctly decoded pulses have sufficient peak power to be detected as a “1” bit. On the transmitter side, an encoder encodes the pulses by first spatially separating the spectrum of the pulse in N spectral slices. Subsequently, the encoder applies a phase shift of 0 or π to each spectral component, where the set of N 0 s or π phase shifts is the spectral code. Finally, the components are spatially recombined to recover the time domain pulse. If the code consists of uniform 0 's or π 's, then the encoded pulse is the same short pulse as the un-encoded input pulse. However, applying a nonuniform code results in spreading of the pulse in the time domain and,

consequently, a drop in the peak power. At the receiver side, a decoder (same as the encoder but operating in reverse) decodes the encoded pulse. The decoder only restores the phase conditions of the initial unencoded pulse and therefore its pulse shape if the conjugate of the encoding code is used. Since the SPECTS-OCDMA receiver is based on threshold detection, it detects a “1” bit only for the correctly decoded signal with sufficient peak power and renders a “0” for the spread-out pulses.

Fig. 1 shows the layout of the OCDMA encoder chip. The AWG spatially separates the spectral components of an ultra short pulse into eight slices. Then an array of eight electro-optical phase shifters applies the spectral code. Finally, the second AWG combines all spectral slices again and routes the recovered time domain encoded pulse into a single output waveguide. Delay lines are incorporated after the phase modulator array to equalize the optical path lengths of the different spectral components.

The epitaxial wafer was grown by metal organic chemical vapor deposition (MOCVD) process on InP substrate. The structure consists a 500 nm thick n-type waveguiding core layer with photoluminescence wavelength at 1150 nm (1.15Q), a 1500 nm thick p-type cladding layer and a 100 nm thick p-type InGaAs contact layer. The fabrication process of the waveguides starts by defining the waveguide mask with a 270 nm PECVD SiO₂ film deposition, photolithography and pattern definition with a CF₄-O₂ reactive ion etch (RIE). A CH₄-H₂ RIE process then forms the ridge waveguides by etching completely through the waveguiding layer with the SiO₂ etch mask. Subsequently, a lateral regrowth process based on a low pressure Hydride Vapor Phase Epitaxy (HVPE) buries the deep etched waveguide by laterally depositing an Fe doped semi-insulating InP layer seeded by the waveguide sidewalls [6]. The lateral regrowth process has highly enhanced growth rate in the lateral direction and resulted in a gently sloped mesa around the deep-etched waveguide with an excellent planar profile close to the etched waveguide, creating essentially a buried heterostructure (BH) waveguide in a single HVPE regrowth step. The HVPE based BH waveguide fabrication technique has many advantages compared to conventional approaches used for realizing ridge, rib-loaded, or traditional BH for curved waveguides. In general, BH waveguides offer lower loss than dry-etched ridge waveguides, and more repeatable results than dry-etched rib-loaded waveguides without the critical control of the etch depth of shallowly-etched waveguides. Furthermore, the HVPE based BH fabrication technique requires one less regrowth step than the traditional BH fabrication process. The remaining SiO₂ masking material was next removed and a *p*-metal (Ti/Pt/Au) contact was evaporated in a bi-level resist based liftoff process. The backside of the wafer was then lapped to 200 um and n-metal (AuGeNi/Au) deposited. The encoder chip was packaged in a butterfly package to allow programmable electrical access to the phase shifter arrays.

3. Experimental results

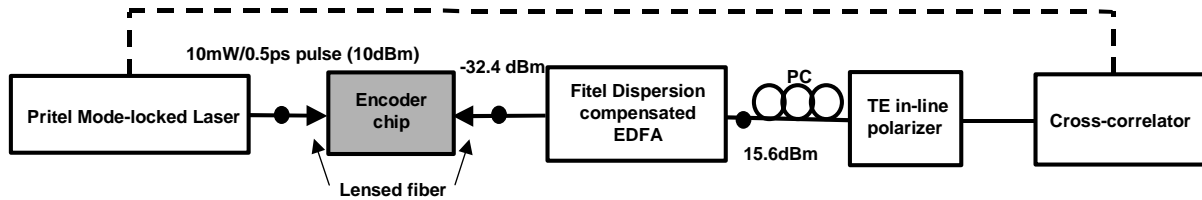


Fig. 3. The experimental setup for characterizing the encoder chip

Fig. 2 shows the transmission spectrum of the O-CDMA encoder. The encoder employed an identical pair of 8-channel AWGs with 180 GHz channel spacing, a measured central wavelength of 1549.2 nm, and a free spectral range (FSR) of 12-channel spacings. The total wavelength span covered by the 8 channels was approximately 1.4 THz, which was sufficient for encoding pulses up to a picosecond. The typical central wavelength mismatch between the AWGs on a single encoder chip was up to 2 nm due to fabrication tolerances. However, using a different input waveguide of the AWG (five are available) provides a shift in the spectral response, which could partially compensate for the mismatch. The phase shifter array consisted of eight 1.5 mm long electro-optical phase shifters based on reverse biased PIN junctions with negligible power consumption (<1 mW). The observed phase shifting was almost a linear function of the reverse bias voltage V_b on the modulators.

Fig. 3 shows the experimental set-up for characterizing the encoder chip. The mode-locked laser generated 0.5 ps pulses with a repetition rate of 10 GHz. A polarization controller (PC) maintained the input signal polarization to transverse electric (TE). Tapered lensed fibers coupled the pulse into and out of the encoder chip. A dispersion compensated EDFA amplified the chip’s output and, finally, a cross-correlator provided time domain characterization.

Encoder experiments used a set of orthogonal 8-bit Walsh codes. Since without applying any coding some initial phase error existed due to fabrication related errors, compensating voltages were applied to the phase shifters to correct for the initial phase coding offset. Walsh codes were then applied in addition to the compensating voltages. The solid curve in Fig. 4(a) shows the measured cross-correlation trace from the encoder chip output with proper phase compensation. A single strong peak was visible with some ringing side peaks at ~ 5 psec period (\sim corresponding to the 180 GHz channel spacing) due to the peaked spectral response of the cascaded AWG filters. Without additional phase coding, the encoder output maintained the short input pulse quite well with a pulse FWHM of 900 fs compared to 500 fs for the original laser pulse. The dashed curve in Fig. 4(a) showed very clearly pulse spreading for Walsh W8 [10010110] coding with 14 V reverse biasing for the '1's and 0V for '0's respectively. Ideally, the "1" in the Walsh code should correspond to π radian phase shift and the "0" should correspond to 0 radian phase shift. Fig. 4(b) shows the corresponding simulation results for the unencoded pulse (solid line) and a W8 coded pulse (dashed line).

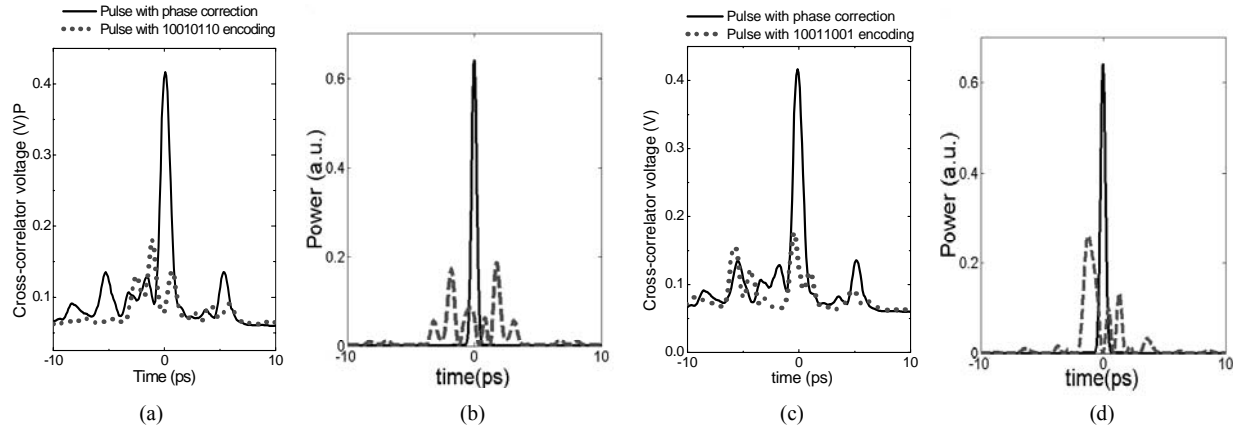


Fig. 4. a) Measured cross-correlation and b) simulated pulse shape results for code W8 [10010110] c) Measured cross-correlation and d) simulated pulse shape results for code W4 [10011001] Solid curves represent unencoded pulses and dotted curves represent encoded pulses.

Fig. 4(c) and 4(d) show the measurement and simulation results are well correlated for Walsh code W4 [10011001]. The simulation results in Fig. 4(d) took into account the initial phase errors extracted from the W8 measurements. The two narrow peaks in the theoretical encoded pulse trace right after $t=0$ (Fig. 4(d)) merged into a single peak in Fig. 4(c), limited by the resolution of the cross-correlator. Fig. 4(c) also shows the ringing peaks with 5 ps period from the AWG spectral slicing, which was not considered in simulation. Overall the simulation and measurement results are in strong agreement, indicating that the integrated encoder chip operated as designed under Walsh Code encoding. The slightly asymmetric profile of the experimental W8 and W4 curves is possibly due to small uncompensated residual phase errors in the encoder chip and power transmission non-uniformities in the eight spectral channels.

4. Summary

We successfully demonstrated spectral encoding of sub-picosecond pulses using a monolithic optical-CDMA encoder/decoder photonic chip using a deep waveguide dry etching /HVPE lateral re-growth based process, which reduces propagation loss and achieves planarization in a single regrowth step.

Reference:

- [1] J.A. Salehi, A.M. Weiner, and J.P. Heritage, "Coherent ultrashort light pulse code-division multiple access communication systems", J. Lightwave Technol., vol. 8(3), pp. 478-491, 1990.
- [2] H. P. Sardesai, C. C. Chang, and A. M. Weiner, "a femtosecond code-division multiple-access communication system test bed," J. Lightwave Technol., vol. 16, no. 11, pp. 1953-1964, 1998.
- [3] R. P. Scott, Wei Cong, Kebin Li, V. J. Hernandez, B. H. Kolner, J. P. Heritage, and S. J. Ben Yoo, "Demonstration of an Error-Free 4x10-Gb/s Multi-User SPECTS O-CDMA Network Testbed", IEEE Photon. Technol. Lett., vol. 16(9) to be published sep. 2004.
- [4] H. Tsuda, H. Takenouchi, T. Ishii, K. Okamoto, T. Goh, K. Sato, A. Hirano, T. Kurokawa, and C. Amano, "Spectral encoding and decoding of 10 Gbit/s femtosecond pulses using high resolution arrayed-waveguid grating, IEE Electron. Lett. vol 35(14), pp. 1186 - 1188, 1999.
- [5] J. P. Heritage, A. M. Weiner, and R. N. Thurston, "Picosecond pulse shaping by spectral phase and amplitude manipulation," Optics Letters, vol. 10, no. 12, pp. 609-11, 1985.
- [6] S.Lourdudoss and O.Kjebon, "Hydride Vapour Phase Epitaxy Revisited," IEEE J. Select. Topics Quantum Electron., 3(3) 749-767 (1997).

This work was supported in part by DARPA and SPAWAR under agreement number N66001-02-1.